UCRL-CONF-213296

Measurement of Molecular Deuterium Fluxes in the DIII-D Edge

E.M. Hollmann, S. Brezinsek, N.H. Brooks, M. Groth, S. Lisgo, A.G. McLean, A. Yu. Pigarov, D.L. Rudakov

June 28, 2005

32nd EPS Plasma Physics Conference
Tarragona, Spain
June 27, 2005 through July 1, 2005

Disclaimer

Measurement of Molecular Deuterium Fluxes in the DIII-D Edge

E.M. Hollmann[1], S. Brezinsek[2], N.H. Brooks[3], M. Groth[4], S. Lisgo[5], A.G. McLean[6],
A.Yu. Pigarov[1], and D.L. Rudakov[1]

[1]*University of California, San Diego, California, USA*
[2]*Forschungszentrum Jülich, Germany*
[3]*General Atomics, San Diego, California, USA*
[4]*Lawrence Livermore National Laboratory, Livermore, California, USA*
[5]*EURATOM, Culham, UK,* [6]*University of Toronto (UTIAS), Toronto, Canada*

In hydrogen-fueled tokamak discharges, the distribution of molecular hydrogen (or deuterium) in the plasma edge region plays a central role in edge fueling, affecting pedestal shape and core density control [1]. In addition to its role in edge fueling, molecular hydrogen is important for plasma edge atomic physics. An example of this is the enhancement of plasma volume recombination known to occur in the presence of vibrationally-excited hydrogen molecules via conversion of H^+ ions into molecular ions such as H_2^+ and H_3^+ [2].

Here, measurements of the D_2 molecule flux into the far edge/scrape-off layer (SOL) of the DIII-D tokamak are made using passive visible spectroscopy of the D_2 diagonal Fulcher band ($3p$-$2s$ triplet Q-branch) line emission over the range $\lambda = 600$–640 nm [3]. L-mode, lower-single-null discharges are studied. A multi-chord visible spectrometer with views of both lower divertor legs and the main chamber is used [4]. A schematic of the spectrometer view chords used here, as well as typical magnetic flux surfaces, midplane probe location, and Thomson scattering view locations, are shown in Fig. 1. As a convenient variable to describe the location of each view chord, the poloidal angle θ of the corresponding emission volume is used (Fig. 1). Each view chord crosses the SOL twice; in the case of the upper view chords and lower view chords, the emission from the SOL closer to the lower divertor is expected to dominate the measured signal. In the case of the midplane view chord, lineshape (Zeeman splitting) analysis of the D_α line indicates that the received emission is typically dominated by the inner wall SOL (over the outer wall SOL by ≈2–8×).

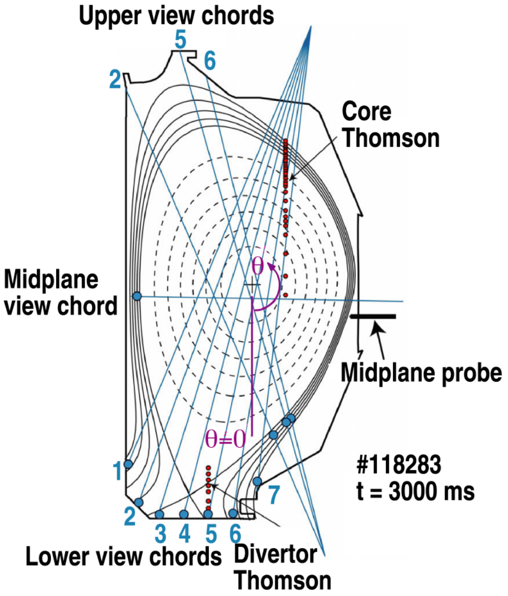

Fig. 1. Schematic of visible spectrometer view chords, midplane probe, and divertor Thomson scattering. Dots indicate approximate emission region locations.

A sample survey of the Fulcher band is shown in Fig. 2 with some of the strongest lines labeled, *e.g.* $Q6(1\text{-}1)$ refers to the $(3p,V'=1,J'=6) \rightarrow (2s,V''=1,J''=6)$ transition, where V and J are the vibrational and rotational quantum numbers. Measured Fulcher band line brightnesses are converted into edge D_2 fluxes by summing over lines to estimate the total band brightness and then multiplying the total band brightness by a *D/XB* (dissociation events per Fulcher photon) conversion factor. Summing over line brightnesses is typically done by fitting to a different rotational temperature for each vibrational level in the excited (3*p*) electronic state and then to a single vibrational temperature to describe the (rotationally summed) level densities in the ground (1*s*) electronic state [5]. The ground electronic state vibrational level densities are mapped to the 3*p* state in the coronal approximation using the vibrationally-resolved Franck-Condon matrix for electron-impact excitation [6]. Typically, these functional forms are found to describe the measured line brightnesses reasonably well. Sample fits are shown in Fig. 3(a) for the 3*p* state rotational temperature for the first two 3*p* state vibrational levels; and in Fig. 3(b) for the 1*s* state vibrational temperature for first 4 vibrational levels (*V*=0 to *V*=3). Off-diagonal (*P* and *R*) branches are not fit explicitly, but are accounted for using a factor 2 correction. In some cases, particularly in detached divertor measurements, a two rotational temperature (bi-Boltzmann) fit is found to better match the 3*p*(*V*=0) brightness data, with the “knee” in the distribution typically occurring around *Q*7.

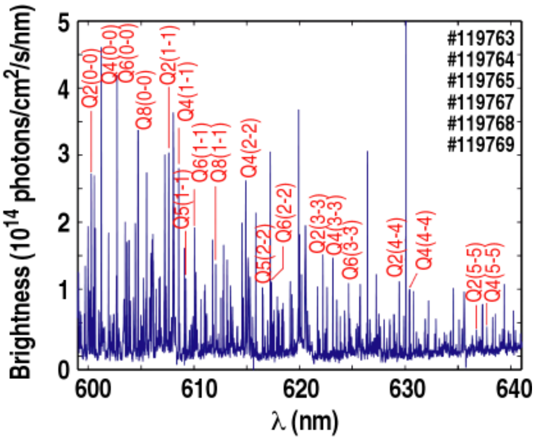

Fig. 2. Survey of D_2 Fulcher band (composite of six spectra using divertor view chord 6).

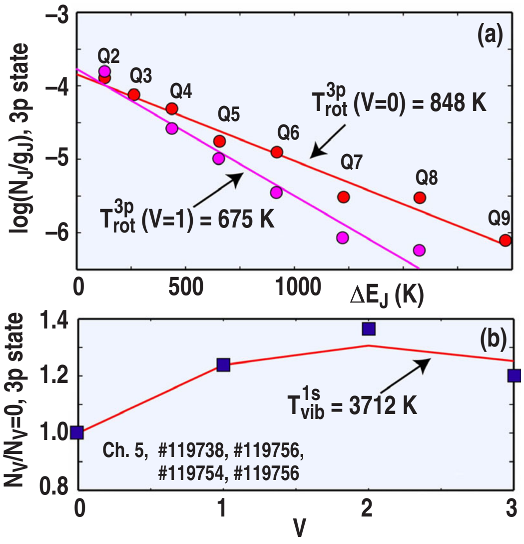

Fig. 3. (a) Single rotational temperature fits to first two vibrational levels of Fulcher band and (b) single-vibrational temperature fit to relative densities of first four vibrational levels.

In DIII-D, measurable line emission has been observed up to the 6th vibrational level (*V*=5) of the Fulcher band. Often, however, it is not practical to measure the entire band, so only the first (*V*=0) branch is measured. In this case, the empirical scaling for T_{vib}^{1s} vs $T_{rot}^{3p}(V=0)$ found in TEXTOR hot edge plasmas with $T_e > 30$ eV can be used to estimate the entire band brightness [7]. In DIII-D, this empirical scaling has been extrapolated to higher n_e and lower T_e conditions, and is typically found to estimate the total band brightness within ±50% for normal (attached) conditions and within $\approx 2\times$ for detached divertor conditions.

Figure 4 shows the measured Fulcher band brightnesses (estimated from the *V*=0 branch) as a function of emission volume poloidal angle θ (with $\theta = 0$ roughly corresponding to the divertor floor, $\theta = \pm.1.5$ to the outer/inner midplane, see Fig. 1). The three cases shown differ primarily in plasma density, the magnetic geometry being nearly identical. As expected, the Fulcher brightness is largest near the divertor strike points, although some signal is still observed in the outer and inner main chamber regions. Blue circles in Fig. 4 are D_α brightness measured during the same discharges using D_α filterscopes. The filterscope view chord geometries are similar to the spectrometer view chords shown in Fig. 1.

Green diamonds in Fig. 4 show the D_α brightnesses predicted to result from D_2 breakup processes. In the midplane view chord (θ = -1.5), where there is almost certainly no recombination, the atomic deuterium in the SOL can be reasonably well accounted for from D_2 breakup. In the divertor region, however, atomic deuterons appear to be $\approx 2-3\times$ more abundant than predicted. This divertor D flux could arise from thermal release of D from hot spots in the divertor floor. However, IR thermography indicates that the divertor remains fairly cold (T_wall < 500 K) in these L-mode discharges and measurements made in front of a graphite test limiter indicate that, for cold (T_wall < 1000 K) wall conditions, deuterons released from graphite are dominantly (>90%) in the form of D_2 neutrals (as opposed to thermal release D or reflection of D^+) [8]. Alternately, at least in Fig. 3(b) and 3(c), the excess D_α emission could be arising from volume recombination processes in the divertor, as DIII-D L-mode plasmas with $n_{e,0} > 2\times10^{13}\text{cm}^{-3}$ are typically expected to begin detaching in at least one divertor leg.

The D/XB factor used to convert measured Fulcher brightnesses into D_2 fluxes is obtained from an experimentally verified [5] collisional-radiative model [9] and increases with both electron density n_e (roughly logarithmically) and with electron temperature T_e (with a minimum at 5 eV and then increasing roughly linearly above 10 eV). Both experiments [7] and simulations [10] indicate that the rotational temperature of the neutral molecules depends dominantly on the electron density, and only weakly on the electron temperature. Here, we use the roughly linear scaling observed in the experiments to estimate the electron density in the Fulcher band emission region from the measured value of $T_{rot}^{3p}(V=0)$. Subsequently, the electron temperature in the emission region is interpolated from the measured edge probe and main chamber Thomson (n_e,T_e) profile (or from the divertor Thomson (n_e,T_e) profile for divertor views). Typically, values of $T_{rot}^{3p}(V=0)\approx$ 600–900 K are measured in the main chamber; corresponding emission region parameters are estimated to be in the range $n_e \approx 0.2\text{-}1.0\times10^{13}\text{cm}^{-3}$ and $T_e \approx 20-60\,\text{eV}$. The local deuteron fueling resulting from D_2 influx can now be estimated as being: $\Gamma_D(D_2) \approx I_{D2}(D/XB)$, where I_{D2} is the

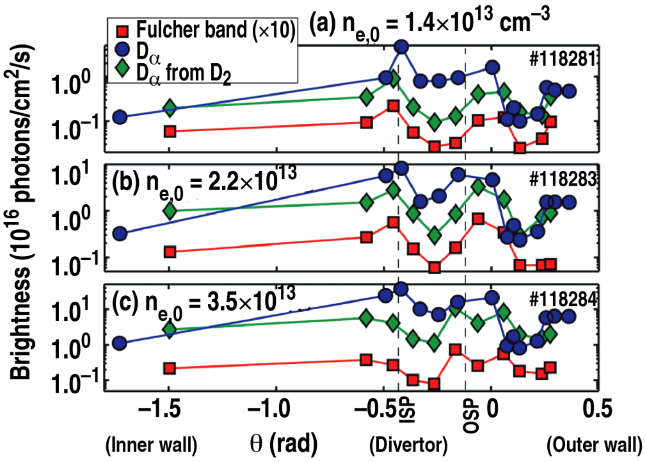

Fig. 4. Fulcher band brightness, D_α brightness, and D_α brightness predicted from D_2 breakup as a function of poloidal angle θ for three different discharge densities.

total Fulcher band brightness. Note that only half of the incident deuterons from each D_2 molecule are assumed to contribute to the fueling flux, *i.e.* we assume that half the deuterons from D_2 result in D atoms which are not ionized but return directly to the chamber wall. Similarly, the local deuteron fueling estimated from D_α emission can be estimated as being: $\Gamma_D(D_\alpha) \approx I_{D\alpha}(S/XB)$, where $I_{D\alpha}$ is the measured D_α brightness and $S/XB \approx 10-20$ is the D ionizations per D_α photon ratio [11]. For the purposes of evaluating S/XB, the D_α emission is assumed to be localized to the same (n_e, T_e) region as the D_2 emission in the same view chord.

In Fig. 5, red squares show fueling (deuteron) flux calculated from the Fulcher band brightnesses of Fig. 4. It can be seen that the recycling flux increases strongly with increasing plasma density, with the maximum flux in the highest central density ($n_{e,0}$ = 3.5× 10^{13} cm^{-3}) case being ≈15× larger than the maximum in the lowest density case ($n_{e,0} = 1.4 \times 10^{13} \text{cm}^{-3}$), consistent with a $n_{e,0}^3$ scaling.

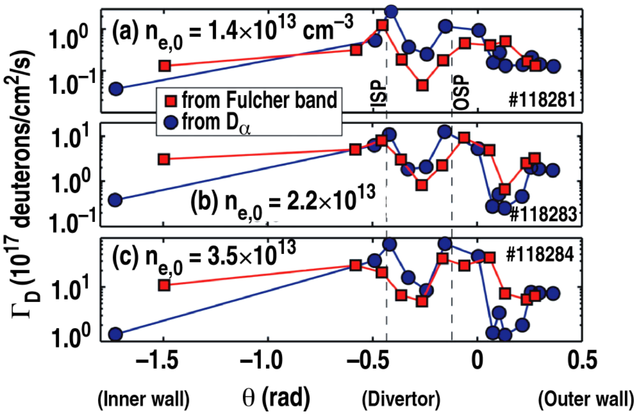

Fig. 5. Deuteron fueling flux from Fulcher band and from D_α vs poloidal angle θ for data of Fig. 4.

The blue circles of Fig. 5 show the apparent deuteron flux resulting from D_α. It can be seen that the main chamber fueling is, on average, underestimated by a factor of roughly 2-3 by measuring D_α only. This is consistent with previous measurements in JET which found that estimates of the deuteron flux from the wall using only the D_α brightness can lead to significant (≈ 2 ×) underestimates [12].

This work was supported by the U.S. Department of Energy under DE-FG02-04ER54758, DE-FC02-04ER54698, and W-7405-ENG-48.

[1] B. Unterberg, S. Brezinsek, G. Sergienko, *et al.,* J. Nucl. Mater. **337**, 515 (2005).
[2] A. Yu. Pigarov, Phys. Scripta **T96**, 16 (2002).
[3] D.K. Otorbae, M.J. de Graaf, M.C. van de Sanden, et al., Contr. Plasma Phys. **35**, 195 (1995).
[4] N. Brooks, D. Fehling, D. Hillis, *et al.,* Rev. Sci. Instrum. **68**, 978 (1997).
[5] S. Brezinsek, P.T. Greenland, P. Mertens, *et al.,* J. Nucl. Mater. **313**, 967 (2003).
[6] U. Fantz and B. Heger, Plasma Phys. Control. Fusion **40**, 2023 (1998).
[7] S. Brezinsek, "Study of atomic and molecular hydrogen in front of a graphite surface in a high-temperature edge plasma," PhD thesis (Forschungszentrum Juelich, 2002).
[8] S. Brezinsek, G. Sergienko, A. Pospiezczyk, *et al.,* to appear in Plasma Phys. Control. Fusion (2005).
[9] P.T. Greenland, Contrib. Plasma Phys. **42**, 608 (2002).
[10] E.M. Hollmann, A.Yu. Pigarov, and K. Taylor, J. Nucl. Mater. **337**, 451 (2005).
[11] H.P. Summers, Atomic Data and Analysis Structure – User's Manual, JET Joint Undertaking Report JET-IR94, 1994.
[12] A. Pospieszczyk, S. Brezinsek, G. Sergienko, *et al.*, J. Nucl. Mater. **337**, 500 (2005).

This work was performed under the auspices of the U.S. Department of Energy by the University of California, Lawrence Livermore National Laboratory under Contract No.W-7405-Eng-48.